PAPER

Check for updates

A nucleic acid-based magnetic potentiometric aptasensing platform for indirect detection of prostate-specific antigen with catalytic hairpin assembly

Shuo Tian, Lingting Huang, Yuan Gao, Zhichao Yu and Dianping Tang [iD] *

In this work, a new nucleic acid-based magnetic potentiometric aptasensing platform was designed for *in situ* amplified measurement of prostate-specific antigen (PSA) with the catalytic hairpin assembly (CHA). The nucleic acid biosensor was constructed by immobilizing thiolated hairpin DNA1 (HP1) on a screen-printed gold electrode (SPGE). PSA-specific aptamers were conjugated onto magnetic beads through the avidin–biotin reaction, followed by hybridization with partially complementary DNA (cDNA). Introduction of target PSA could cause the detachment of cDNA from magnetic beads because of the PSA–aptamer reaction. The detached cDNA opened the immobilized HP1 on the SPGE to induce the catalytic hairpin assembly between HP1 and hairpin DNA2 (HP2), thereby resulting in the recycling of cDNA for repeated utilization. In this case, numerous HP1 and HP2 probes were opened to form many double-stranded DNA molecules on the electrode. Relative to the HP1-modified SPGE, the electric potential was shifted before and after hybridization with HP2. Under optimum conditions, the potential shift was proportional to the PSA concentration within the dynamic range of 0.01–30 ng mL^{-1}, and the limit of detection was estimated to be 9.3 pg mL^{-1} PSA. The reproducibility with the inter-assay and intro-assay was below 10.58% (RSD). Good specificity and long-term stability were acquired for PSA measurement. Importantly, the method accuracy of nucleic acid-based magnetic potentiometric aptasensing was acceptable for analysis of human serum samples in comparison with that of reference human PSA ELISA kits.

Key Laboratory for Analytical Science of Food Safety and Biology (MOE & Fujian Province), Department of Chemistry, Fuzhou University, Fuzhou 350108, People's Republic of China. E-mail: dianping.tang@fzu.edu.cn

Introduction

An aptamer (an oligonucleotide sequence of DNA or RNA, XNA, or peptide) is usually obtained from a library of nucleic acids through an *in vitro* screening technique (*i.e.*, systematic evolution of ligands by exponential enrichment, SELEX).[1] Thanks to specifically binding with different molecules (*e.g.*, cancer biomarkers, small molecules, metal ions and so on), aptamers have been widely applied in analytical fields.[2,3] The enzyme-linked immunosorbent assay (ELISA) method plays an important role in the detection of various biological molecules, and many kits on the market have been developed on the basis of this principle.[4,5] However, the corresponding antibodies as biosensing probes are relatively expensive and easy to denature through environmental factors such as pH and temperature.[6] In contrast, aptamers are smaller than proteins, easy to synthesize, stable, and have the same

sensitivity as antigen–antibody reactions.[7,8] Therefore, aptamers are expected to replace the conventional ELISAs and become powerful tools for the detection of various biomolecules.

Recently, different aptasensing protocols have been reported and developed for analysis and quantification of biomolecules.[9–11] Mahjub *et al.* constructed a label-free colorimetric aptasensing approach for the detection of tobramycin in milk based on a cationic polymer and silver nanoparticles.[12] Zeng *et al.* presented an engineered palindromic molecular beacon based Z-scheme photoelectrochemical aptasensing platform for the selective screening of kanamycin.[13] Mohammadi *et al.* developed an electrochemical aptasensing platform for solvated mercuric ions based on gold nanoparticle-coated MoS_2 multiwalled carbon nanotubes.[14] Recent studies have looked at developing innovative and powerful aptasensing schemes for detection of disease-related proteins, *e.g.*, carcinoembryonic antigen (CEA),[15] and prostate-specific antigen (PSA).[16] Loyez *et al.* summarized recent advances on optical fiber aptasensing systems over the last decade for the detection of biomarkers at extremely low concentrations and in small volumes.[17] Kou *et al.* highlighted recent advances in optical

platform-based sensing strategies for cancer diagnostics using aptamers.[18] Introduction of aptamers gave a low-cost sensing design and a similar analytical performance to antibody-based assays.

For the successful development of aptamer-based cancer diagnostics, an important aspect is how to achieve an *in situ* amplified detectable signal through various signal-transduction methods.[19,20] Potentiometers (*i.e.*, pH meter) are currently one of the most widely used devices in the world because of their portable size, easy operation, low cost and reliable quantitative results.[21] Potentiometric measurements are often carried out with a two-electrode system including a working electrode and reference electrode without external excitement such as current and voltage.[22] Gao *et al.* introduced a versatile approach to carry out potentiometric aptasensing of *Escherichia coli* by electrogenerated chemiluminescence.[23] To the best of our knowledge, a few reports were focused on the potentiometric measurement of cancer biomarkers.[24–28] One of the major bottlenecks for potentiometric aptasensors is how to amplify the detectable signal. Catalytic hairpin assembly (CHA; an enzyme-free amplification method) has been proven to be useful in amplifying the transducing signals at the terminus since it could yield a hundred-fold catalytic amplification with a negligible background and the transducer analyte binding to various detection modalities.[29] In this regard, CHA can be employed as the specific end-point transducer for development of isothermal amplification strategies.[30] To this end, our motivation in this study is to utilize the CHA-based amplification strategy for fabrication of a potentiometric aptasensing platform to determine disease-related proteins.
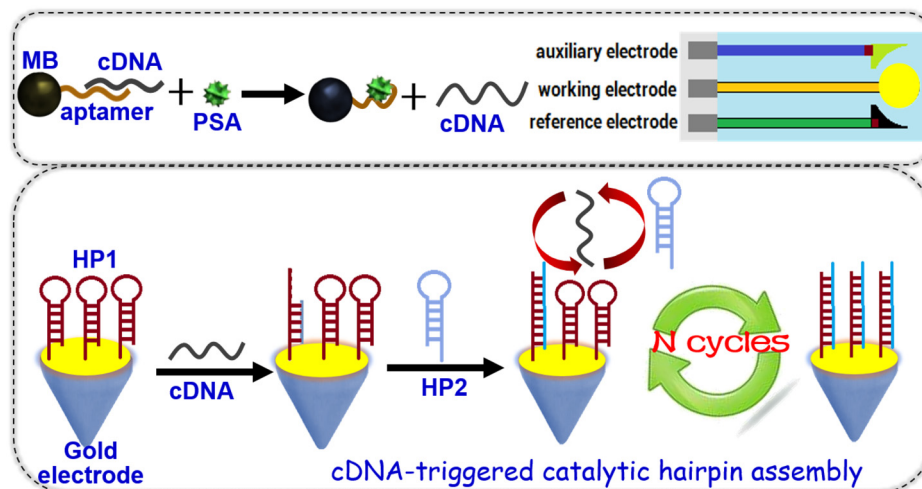
Prostate-specific antigen (PSA) belongs to the serine protease family with tissue specificity and a chymotrypsin-like effect, and decomposes the main gelatinous protein in semen and dilute semen.[31] Elevated serum PSA is seen in pathological conditions of the prostate, such as prostatitis and benign prostatic hyperplasia.[32] Herein, we devise a magnetic potentiometric aptasensing platform for indirect detection of PSA with catalytic hairpin assembly (Scheme 1). This system involves two hairpin DNA probes, complementary DNA and PSA-specific aptamers. The dissolution of complementary DNA by the target PSA triggers catalytic hairpin assembly between hairpin DNA1 and hairpin DNA2. The recycling of complementary DNA can amplify the detectable signal *via* the shift in the electrode potential before and after hybridization of hairpin DNA1 with hairpin DNA2. The major objective of this work is to construct a new potentiometric aptasensing system for the analysis of low-abundance proteins with high sensitivity and specificity.

Experimental section

Materials and reagents

Human PSA standards were purchased from AmyJet Sci. Inc. (Wuhan, China). All the oligonucleotides used in this study were acquired from Sangon Biotech. Co., Ltd. (Shanghai, China) as follows: PSA-specific biotinylated aptamer: 5′-biotin-$(T)_{10}$-ATTAAAGCTCGCCATCAAATAGC TGC-3′, partially complementary DNA with PSA aptamer (cDNA): 5′-CGACAT CT AACCTAGCTCACTGACGCAGCTATTT-3′, hairpin DNA1 (HP1): 5′-SH-GTCAGTGAGCTAGGTTAGATGTCGCCATGTGTAG ACGACA TCTAACCTAGC-3′, and hairpin DNA2 (HP2): 5′-AGATGTCGTCTACACATGG CGACATCTAACCTAGCCCATGTGT AGA-3′ (note: the sequences of these oligonucleotides were designed by consulting these two studies[16,33]). Prior to the experiment, we used RNA folding prediction software to simulate the designed DNA structures for the formation of DNA hairpins (software: web servers for RNA secondary structure prediction, Mathews Lab, **https://www.rna.urmc.**

Scheme 1 Schematic illustration of the nucleic acid–based magnetic potentiometric aptasensing system for the quantitative monitoring of prostate–specific antigen (PSA) by coupling with catalytic hairpin assembly (CHA) on a hairpin DNA1 (HP1)–coated screen-printed gold electrode (SPGE) (cDNA: partially complementary DNA; HP2: hairpin DNA2; MB: magnetic bead).

rochester.edu). Streptavidin magnetic beads (Cat no.: HY-K0208; 10 mg mL^{-1}; mean diameter: 1.0 μm; bind capacity for biotinylated oligonucleotides: >500 pmol mg^{-1}) were obtained from MedChemExpress Inc. (Shanghai, China). All the screen-printed gold electrodes were obtained from Taobao (Weihai, China), which comprised a 4.0 mm gold working electrode, carbon counter electrode and Ag/AgCl reference electrode. 6-Mercaptohexanol (MCH) was obtained from Sigma-Aldrich (Shanghai, China). Ultrapure water was obtained from a Millipore water purification system (18.2 MΩ cm, Milli-Q, Millipore). All the other chemicals were of analytical grade, and used without further purification. All the buffers, including phosphate-buffered saline (PBS; 10 mM, pH 7.4) solution, were prepared according to guidelines. Tris-HCl buffer (10 mM, pH 7.5) contained 1.0 mM EDTA, 1.0 M NaCl and 0.1% Tween-20.

Binding of biotinylated aptamers with streptavidin magnetic beads

The biotinylated aptamers were conjugated to streptavidin magnetic beads on the basis of the avidin–biotin reaction. Initially, the purchased magnetic beads were suspended on a mixer for vortex oscillation for 20 s. Then, 100 μL of 10 mg mL^{-1} magnetic beads were injected into a 1.5 mL centrifuge tube and magnetically separated on a magnetic rack, and the supernatant was discarded. The collected magnetic beads were washed twice with 1.0 mL of Tris-HCl buffer (10 mM, pH 7.5). Following that, 500 μL of 10 μM aptamers dispersed in the above Tris–HCl buffer was added to the magnetic beads, and incubated (30 min at room temperature and 2 h at 4 °C) on a rotary mixer. The resulting suspension was separated magnetically and washed as before. Aptamer-conjugated magnetic beads (designated as Apt-MB) were dispersed into 500 μL of Tris-HCl buffer (10 mM, pH 7.5) at an Apt-MB concentration of ~2.0 mg mL^{-1} for use.

Preparation of the hairpin DNA1-modified screen-printed electrode

The thiolated hairpin DNA1 probes were modified onto a screen-printed gold electrode (active area: 12.56 mm^2) through typical Au–S bonds. Firstly, the purchased screen-printed gold electrode was washed by sonication in ultrapure water and ethanol for 5 min, respectively. Then, the resulting electrode was scanned in 0.5 M deoxygenated H$_2$SO$_4$ with applied potentials from −0.3 to 1.5 V at 50 mV s^{-1} until a voltammogram characteristic of a clean gold electrode was established. After thorough rinsing with ultrapure water and ethanol, 100 μL of 10 μM thiolated aptamers were thrown on the working electrode, and incubated for 60 min at room temperature. After that, the resulting electrode was washed as before. 100 μL of 1.0 mM 6-mercaptohexanol in 10 mM Tris-HCl buffer (pH 7.5) was dropped on the electrode and reacted for 60 min at room temperature to block possible active sites and avoid non-specific adsorption. Finally, the

hairpin DNA1-modified screen-printed gold electrode (HP1/SPGE) was stored at 4 °C for subsequent usage.

Analytical process and potentiometric measurements

Scheme 1 gives a schematic illustration of the nucleic acid-based magnetic potentiometric aptasensing platform for the indirect determination of PSA with catalytic hairpin assembly. Prior to measurement, Apt-MB was initially hybridized with complementary DNA (cDNA) via adding 500 μL of 25 μM cDNA (excess) (note: The reason for using excess cDNA was to ensure an adequate hybridization reaction with the conjugated aptamers on magnetic beads for formation of cDNA/Apt-MB) into the Apt-MB suspension (500 μL, 2.0 mg mL^{-1}) in Tris-HCl buffer (10 mM, pH 7.5) and reacted for 2.0 h at 37 °C to form cDNA/Apt-MB conjugates. After magnetic separation, the collected cDNA/Apt-MB conjugates were dispersed in 500 μL of Tris-HCl buffer (10 mM, pH 7.5) (Conc.$_{[cDNA/Apt-MB]}$ ≈ 2.0 mg mL^{-1}). Following that, 50 μL of PSA standard/sample at a certain level was mixed with 50 μL of cDNA/Apt-MB conjugates (2.0 mg mL^{-1}), and incubated for 70 min at 37 °C with slight shaking on a shaker. During this process, target PSA was specifically bound with the aptamer to release the cDNA. The supernatant after magnetic separation was dropped on the HP1/SPGE (note: The supernatant should contain the released cDNA and excess PSA protein, which should be discussed for non-specific adsorption in the subsequent work). Meanwhile, 50 μL of 25 μM hairpin DNA2 (HP2, excess) was added to the mixture, and incubated for 90 min at 37 °C to carry out the catalytic hairpin assembly. After washing with Tris-HCl buffer (10 mM, pH 7.5), the resulting electrode (i.e., HP2-HP1/SPGE) was measured in Tris-HCl buffer (10 mM, pH 7.5) by potentiometry with a two-electrode system including the HP2-HP1/SPGE working electrode and an Ag/AgCl reference electrode. The electrode potential (mV) was collected and registered as the sensing signal toward different concentrations of PSA standard/sample. All measurements were carried out at room temperature (25 ± 1.0 °C). Analyses were always made in triplicate.

Results and discussion

Design and characterization of electrochemical aptasensor

In this work, PSA-specific aptamers were labeled onto the surface of magnetic beads through the classical avidin–biotin reaction between PSA-specific biotinylated aptamers and streptavidin magnetic beads. To fabricate the electrochemical sensing system, thiolated HP1 probes were modified onto the surface of a screen-printed gold electrode via Au–S bonds. In the presence of target PSA, the analyte specifically reacted with the labeled aptamer on a magnetic bead. In this case, the complementary DNA was released from the magnetic bead, which could readily open the hairpin DNA1 probe to implement the catalytic hairpin assembly upon addition of hairpin DNA2. In this case, the electrical potential (EMF) of the modified SPGE was changed before and after the catalytic

hairpin assembly. By monitoring the shift in the EMF, we could quantitatively determine the concentration of target PSA in the sample.

To realize our design, one crucial issue was whether the released cDNA could readily open hairpin DNA1. To demonstrate this concern, we used agarose gel electrophoresis to monitor the reaction. The results indicated that hairpin DNA1 could be opened through hybridization reaction with cDNA. Furthermore, the progression of catalytic hairpin assembly was investigated with gel electrophoresis by mixing cDNA, hairpin DNA1 and hairpin DNA2, acquiring an expected experimental result. Significantly, cDNA and hairpin DNA1 could not hybridize with hairpin DNA2 alone, indicating that the catalytic hairpin assembly was derived from the released cDNA in the presence of HP1 and HP2. Note: to avoid the possible overlapping with our previous work and the repeated description, the experimental results were not shown in this study. Please see our previously published work.[16]

Logically, another important concern arises about whether thiolated hairpin DNA1 probes could be immobilized onto the screen-printed gold electrode. To clarify this point, we employed a high-resolution inverted microscope to investigate the gold electrode before and after modification with thiolated hairpin DNA1 (Fig. 1). Fig. 1A gives a typical microscopy image of the cleaned gold electrode. When the thiolated hairpin DNA1 probes were modified onto the electrode, however, the gold surface became rougher than that of the cleaned gold electrode (Fig. 1B). Therefore, thiolated hairpin DNA1 could be modified onto the screen-printed gold electrode through Au–S bonds.

Electrochemical characterization and feasibility evaluation

In this system, the electrical potential was acquired on the basis of the released cDNA, which triggered catalytic hairpin assembly on the HP1-modified SGPE. Because of specific PSA–aptamer reaction, the complementary cDNA could be dissociated from the aptamer/cDNA in the presence of target PSA. Logically, one puzzling issue is whether cDNA could cause the catalytic hairpin assembly on the modified electrode. To verify this issue, we used electrochemical impedance spectroscopy (EIS) to investigate this process on
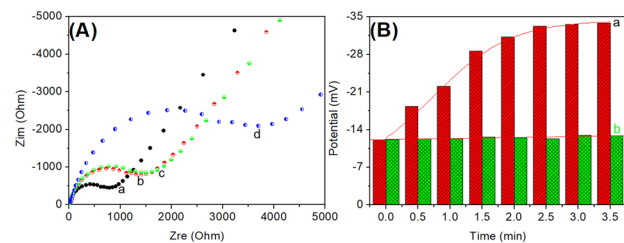

Fig. 2 (A) Nyquist diagrams of (a) SPGE, (b) HP1/SPGE, (c) cDNA-HP1/SPGE and (d) cDNA-HP1/SPGE after catalytic hairpin assembly in PBS (10 mM, pH 7.4) containing 2.5 mM $Fe(CN)_6^{4-/3-}$ and 0.1 M KCl within the range of 10^{-2} to 10^5 Hz at an alternating voltage of 5.0 mV; (B) potential responses (mV, *versus* reaction time) of the developed potentiometric aptasensor in the (a) presence and (b) absence of target PSA (1.0 ng mL^{-1} used in this case).

HP1-modified SPGE in pH 7.4 10 mM PBS containing 2.5 mM $Fe(CN)_6^{4-/3-}$ and 0.1 M KCl (Fig. 2A). Typically, the diameter of the semicircle in a Nyquist diagram is equivalent to the electron transfer resistance (R_{et}, ohms). Curve 'a' represents a typical Nyquist diagram of the cleaned SPGE, and a small resistance was achieved. After modification with HP1, the resistance of HP1/SPGE became large (curve 'b'). The increased resistance was mainly derived from the negatively charged phosphate groups on the oligonucleotides, which repulsed the negatively charged $Fe(CN)_6^{4-/3-}$. When the as-prepared HP1/SPGE reacted with cDNA, the resistance generally increased (curve 'c'). The reason might be the fact that the resistance of hairpin HP1 (loop region) was almost the same as that of the partially complementary double-stranded DNA. Significantly, the resistance increased again after the catalytic hairpin assembly with HP2 (curve 'd'), indicating the formation of double-stranded DNA. These results revealed that the prepared HP1/SPGE could be utilized for the catalytic hairpin assembly during the measurement.

To further investigate the feasibility of this method, the prepared Apt-MB and HP1/SPGE were employed for the detection of PSA (1.0 ng mL^{-1} used as an example) with potentiometric measurement in Tris-HCl buffer (10 mM, pH 7.5) under different conditions (Fig. 2B). Column 'b' gives the electrical potentials of the magnetic potentiometric aptasensing system in the absence of target PSA, and the
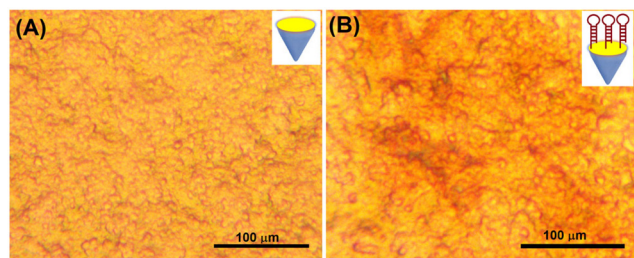

Fig. 1 Microscopy images of (A) the cleaned screen-printed gold electrode and (B) HP1-modified screen-printed gold electrode.
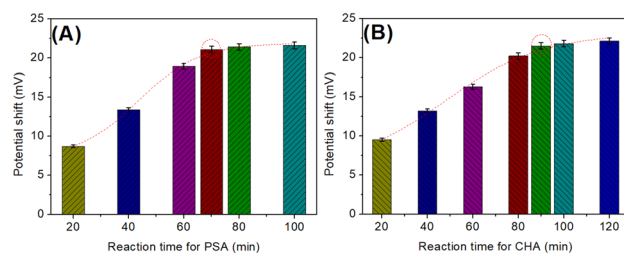

Fig. 3 Dependence of potentials (ΔmV relative to the background signal) of the potentiometric aptasensor on the (A) reaction time of cDNA/Apt-MB with target PSA, and (B) reaction time for CHA (1.0 ng mL^{-1} PSA used as an example).
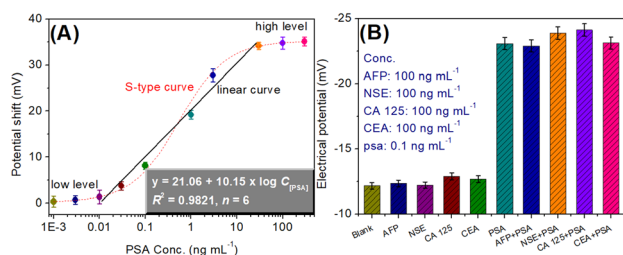
Fig. 4 (A) Potential change (*versus* background signal) of the magnetic potentiometric aptasensing method toward PSA standards; (B) the specificity of the magnetic potentiometric aptasensing system toward AFP, NSE, CA 125, CEA and PSA.

steady-state potential was about −12.2 mV. After the cDNA-Apt/MB reacted with 1.0 ng mL^{-1} PSA, the electrical potential of the formed HP2-HP1/SPGE became −33.2 mV (column 'a'). The shift in the potential was mainly derived from the formed double-stranded DNA with a negative charge. These results indicated that the magnetic potentiometric aptasensing platform could be preliminarily applied for detection of target PSA.

Optimization of experimental conditions

To acquire an optimal analytical performance, some experimental conditions, *e.g.*, reaction time of cDNA/Apt-MB with target PSA, and time for the catalytic hairpin assembly, should be investigated. Note: 1.0 ng mL^{-1} PSA was used as an example for condition optimization. During the measurement, the signal intensity mainly depended on the released cDNA in the presence of target PSA. Fig. 3A shows the change in the electrical potential of the developed potentiometric aptasensing system relative to different reaction times between cDNA/Apt-MB and target PSA. The detectable signal increased with increased reaction time, and tended to level off after 70 min. A longer reaction time did not cause a significant increase. To save time for the assay, 70 min was used for the reaction of cDNA/Apt-MB with target PSA in this study.

By the same token, we also investigated the effect of the catalytic hairpin assembly time on the electrical potential of the potentiometric aptasensing platform. As shown in Fig. 3B, an optimal electrical potential was achieved after 90 min. The results indicated that the reaction of HP1/SPGE

with HP2 and cDNA could reach a dynamic equilibrium. Similarly, 90 min was selected for the catalytic hairpin assembly.

Analytical performance of potentiometric aptasensing toward PSA

By using the as-prepared cDNA/Apt-MB and HP1/SPGE, target PSA standards with different concentrations were determined under the optimum conditions. The signal was collected on the basis of the shift in the electrical potential relative to background EMF. Fig. 4A gives the relationship between the potential shift and the logarithm of PSA concentration. Within the ranges of PSA standards at low levels (from 0.001 to 0.01 ng mL^{-1}) or high concentrations (from 30 to 300 ng mL^{-1}), the shift in the electrical potential was not obvious. Significantly, a good linear relationship between the potential shifts and the logarithm of PSA concentrations could be achieved in the dynamic range from 0.01 to 30 ng mL^{-1}. The regression equation could be fit as y (mV) = 21.06 + 10.15 × log $C_{[PSA]}$ (ng mL^{-1}, R^2 = 0.9821, n = 6). The limit of detection (LOD) could be estimated to be 9.3 pg mL^{-1} on the basis of $3S/K$ (where S stands for the slope of linear curve, and K is the standard deviation of 13 blank samples). Moreover, the linear range and LOD of our system were comparable with those of other PSA analytical methods with a potential readout (Table 1).

Specificity, reproducibility and storage stability

The specificity of the potentiometric aptasensing system was monitored for the analysis of other non-target PSA proteins or biomarkers, *e.g.*, alpha-fetoprotein (AFP), neuron-specific enolase (NSE), cancer antigen 125 (CA 125) and carcinoembryonic antigen (CEA). As seen from Fig. 4B, the electrical potentials of the modified HP1/SPGE were almost the same toward these non-target analytes. However, the electrical potential was obviously higher in the presence of target PSA. These results indicated that our developed potentiometric aptasensing system had good selectivity toward target PSA.

Further, the reproducibility of the potentiometric aptasensing system was evaluated toward three PSA standards by using the same-batch or various-batch cDNA/Apt-MB and HP1/SPGE, respectively. Table 2 gives the

Table 1 Comparison of analytical properties of the potentiometric aptasensing with other PSA potentiometric analytical methods (*e.g.*, linear range and LOD)

Method	Linear range	LOD	Ref.
Potentiometric immunoassay	4.0–13 ng mL^{-1}	3.4 ng mL^{-1}	34
Potentiometric immunoassay	0.1–50 ng mL^{-1}	0.1 ng mL^{-1}	35
Potentiometric immunoassay	0.5–18 ng mL^{-1}	0.1 ng mL^{-1}	36
Potentiometric immunoassay	0.1–50 ng mL^{-1}	0.04 ng mL^{-1}	37
Potentiometric immunoassay	2.6–59.4 ng mL^{-1}	2.0 ng mL^{-1}	38
Potentiometric immunoassay	0.05–20 ng mL^{-1}	13.6 pg mL^{-1}	39
Potentiometric aptasensing	0.01–30 ng mL^{-1}	9.3 pg mL^{-1}	This work

Table 2 Reproducibility of the potentimetric aptasensor for the various sensors with the same-batch or different-batch preparation (Conc. units: ng mL^{-1})

	Conc.	1st assay	2nd assay	3rd assay	RSD (%)
Intra-assay	0.05	0.056	0.046	0.052	9.81
	1.0	1.04	0.96	1.12	7.69
	20.0	18.9	21.1	19.7	5.95
Inter-assay	0.05	0.056	0.046	0.048	10.58
	1.0	0.94	1.08	1.13	9.38
	20.0	21.5	22.4	18.4	10.11

Table 3 Analysis of real human serum specimens with the magnetic potentiometric aptasensor and commercialized human PSA ELISA kit

Sample no.[a]	Method, Conc. (mean ± SD, ng mL^{-1}, $n = 3$)		t_{exp}
	Aptasensor	ELISA kit	
1	23.11 ± 2.12	21.23 ± 1.36	1.29
2	4.56 ± 0.31	4.89 ± 0.28	1.37
3	13.12 ± 0.12	14.27 ± 0.89	2.22
4	27.12 ± 1.29	25.6 ± 1.65	1.26
5	5.41 ± 0.31	5.23 ± 0.22	0.82
6[b]	0.51 ± 0.019	0.59 ± 0.035	3.48

[a] All samples were diluted with a blank human serum sample within the linear range of the potentiometric aptasensor. [b] Sample #6 was obtained through the dilution of sample #5 to 10-fold.

experimental results. Obviously, the relative standard deviations (RSDs) were 9.81%, 7.69% and 5.59% for the inter-assay with 0.05, 1.0 and 20.0 ng mL^{-1} PSA, respectively, whereas these were 10.58%, 9.38% and 10.11% for the intra-assay toward the corresponding levels, indicating good reproducibility.

Finally, the storage stability of Apt-MB and HP1/SPGE was studied at 4 °C. The evaluation was implemented after storing them at 4 °C for some time, and then 1.0 ng mL^{-1} PSA was determined. The results indicated that the signals of the potentiometric aptasensing system could be maintained at 98.3%, 97.4%, 96.6%, 94.1%, 92.4% and 90.1% of the initial signal after storage for 1, 2, 3, 4, 6 and 8 months, respectively. Thus, the storage stability of Apt-MB and HP1/SPGE at 4 °C was acceptable.

Analysis of human serum samples

The accuracy of the potentiometric aptasensing system was evaluated for the analysis of real human serum samples, which were gifted by the hospital of our university. All the serum samples were measured referring to the above-described process. To study the practical application of the newly developed method, the obtained results from our system were compared with those obtained from a commercialized human PSA ELISA kit. As indicated from Table 3, no significant differences were encountered between the two methods at the 0.05 significance level because all t_{exp}

values were less than 4.30 ($t_{crit\ [0.05,\ 2]}$ = 4.30) (t_{exp}: experimental value; t_{crit}: critical value) by the application of an F-test. To this end, the potentiometric aptasensing method can be preliminarily used for the measurement of target PSA in real samples.

Conclusions

In summary, a simple sensitive potentiometric aptasensing method was designed for quantitative monitoring of a low-abundance disease-related biomarker, PSA, in biological fluids. This system could be carried out by coupling with aptamer-functionalized magnetic beads and a hairpin probe-modified electrode. Relative to traditional PSA electrochemical detection methods, our strategy had the following advantages, e.g., avoiding the participation of expensive antibodies, and no requirement of enzyme labels. Meanwhile, the reaction of the target with the aptamer and potentiometric measurements were executed in two different systems, thereby efficiently decreasing the system interference. Significantly, our system can be extended for the fabrication of other biomarker-specific aptasensing systems by controlling the corresponding aptamer.

Compliance with ethical standards

All experiments were performed in accordance with the Guidelines of Fuzhou University (China), and approved by the ethics committee at Fuzhou University, China. Informed consents were obtained from the human participants of this study.

Author contributions

Shuo Tian: conceptualization, methodology, investigation, and writing – original draft. Lingting Huang: conceptualization, visualization, investigation, and writing – original draft. Zhichao Yu: resources, software, and data curation. Yuan Gao: investigation, validation, formal analysis, and writing – original draft. Dianping Tang: funding acquisition, supervision, and writing – review & editing.

Conflicts of interest

There are no conflicts to declare.

Acknowledgements

References

1 R. Canovas, E. Daems, A. Langley and K. De Wael, *Biosens. Bioelectron.*, 2023, **220**, 114881.

2 J. Pan, W. Xu, W. Li, S. Chen, Y. Dai, S. Yu, Q. Zhou and F. Xia, *Anal. Chem.*, 2023, **95**, 420–432.

3 A. Downs and K. Plaxco, *ACS Sens.*, 2022, **7**, 2823–2832.

4 Z. Luo, L. Zhang, R. Zeng, L. Su and D. Tang, *Anal. Chem.*, 2018, **90**, 9568–9575.

5 L. Huang, J. Chen, Z. Yu and D. Tang, *Anal. Chem.*, 2020, **92**, 2809–2814.

6 B. Zhang, D. Tang, R. Goryacheva, R. Niessner and D. Knopp, *Chem. – Eur. J.*, 2013, **19**, 2496–2503.

7 M. Kohlberger and G. Gadermaier, *Biotechnol. Appl. Biochem.*, 2022, **69**, 1771–1792.

8 A. Miller, A. Rao, S. Nelakanti, C. Kujalowicz, T. Shi, T. Rodriguez, A. Ellington and G. Stovall, *Anal. Chem.*, 2022, **94**, 7731–7737.

9 B. Manuel, S. Sterling, A. Sanford and J. Heemstra, *Anal. Chem.*, 2022, **94**, 6436–6440.

10 M. Negahdary and L. Angnes, *Biomater. Adv.*, 2022, **135**, 112689.

11 Y. Zhao, K. Yavari and J. Liu, *TrAC, Trends Anal. Chem.*, 2022, **146**, 116480.

12 R. Mahjub, O. Shayesteb, K. Derahshandeh, A. Ranjbar, F. Mehri and A. Heshmati, *Food Chem.*, 2020, **382**, 132580.

13 R. Zeng, Z. Luo, L. Su, L. Zhang, D. Tang, R. Niessener and D. Knopp, *Anal. Chem.*, 2019, **91**, 2447–2454.

14 A. Mohammadi, E. Heydari-Bafrooei, M. Foroughi and M. Mohammadi, *Microchem. J.*, 2020, **158**, 105154.

15 S. Lv, K. Zhang, L. Zhu and D. Tang, *Anal. Chem.*, 2020, **92**, 1470–1476.

16 S. Lv, K. Zhang, Y. Zeng and D. Tang, *Anal. Chem.*, 2018, **90**, 7086–7093.

17 M. Loyez, M. DeRosa, C. Caucheteur and R. Wattiez, *Biosens. Bioelectron.*, 2022, **196**, 113694.

18 X. Kou, X. Zhang, X. Shao, C. Jiang and L. Ning, *Anal. Bioanal. Chem.*, 2020, **412**, 6691–6705.

19 X. Pei, B. Zhang, J. Tang, B. Liu, W. Lai and D. Tang, *Anal. Chim. Acta*, 2013, **758**, 1–18.

20 G. Ibanez-Redin, G. Rosso Cagnani, O. Nathalia, P. Raymundo-Pereira, S. Sergio, M. Gutierrez, J. Krieger and O. Oliveira, *Biosens. Bioelectron.*, 2023, **223**, 114994.

21 X. Shang, J. Yu, C. Wang and Y. Du, *Electroanalysis*, 2022, **34**, 535–541.

22 R. Gao, B. Liu, D. Luo, Y. Su and L. Su, *Electroanalysis*, 2022, **34**, 275–280.

23 X. Gao, T. Jiang and W. Qin, *Biosens. Bioelectron.*, 2022, **200**, 113923.

24 Y. Chen, B. Liu, P. Lyu, H. Kwok, L. Ge and Q. Wu, *Anal. Bioanal. Chem.*, 2021, **413**, 1073–1080.

25 G. Li, W. Li, S. Li, X. Shi, J. Liang, J. Lai and Z. Zhou, *Biochem. Eng. J.*, 2020, **164**, 107780.

26 Z. Hong, G. Chen, S. Yu, R. Huang and C. Fan, *Anal. Methods*, 2018, **10**, 5364–5371.

27 G. Zelada-Guillen, A. Tweed-Kent, M. Niemann, H. Goringer, J. Riu and F. Rius, *Biosens. Bioelectron.*, 2013, **41**, 366–371.

28 A. Duzgun, A. Maroto, T. Mairal, C. O'Sullivan and F. Rius, *Analyst*, 2010, **135**, 1037–1041.

29 J. Zhuang, W. Lai, G. Chen and D. Tang, *Chem. Commun.*, 2014, **50**, 2935–2938.

30 H. Gong, X. Hu, R. Zeng, Y. Li, J. Xu, M. Li and D. Tang, *Sens. Actuators, B*, 2022, **369**, 132307.

31 Z. Lv, R. Zeng, L. Zhu, Z. Qiu, M. Li and D. Tang, *Sens. Actuators, B*, 2022, **370**, 132440.

32 G. Cai, Z. Yu, R. Ren and D. Tang, *ACS Sens.*, 2018, **3**, 632–639.

33 C. Jung, P. Allen and A. Ellington, *Nat. Nanotechnol.*, 2016, **11**, 157–163.

34 Y. Liu, *Thin Solid Films*, 2008, **516**, 1803–1808.

35 J. Szucs, E. Pretsch and R. Gyurcsanyi, *Analyst*, 2009, **134**, 1601–1607.

36 X. Wang, G. Tao and Y. Meng, *Electroanalysis*, 2009, **21**, 2109–2115.

37 B. Zhang, B. Liu, G. Chen and D. Tang, *Biosens. Bioelectron.*, 2014, **53**, 465–471.

38 M. Rebelo, C. Santos, J. Costa-Rodrigues, M. Fernandes, J. Noronha and M. Sales, *Electrochim. Acta*, 2014, **132**, 142–150.

39 S. Lv, Z. Lin, K. Zhang, M. Lu and D. Tang, *Anal. Chim. Acta*, 2017, **964**, 67–73.